


SCIENTIFIC REPORTS



OPEN

Administration of *N*-Acyl-Phosphatidylethanolamine Expressing Bacteria to Low Density Lipoprotein Receptor^{-/-} Mice Improves Indices of Cardiometabolic Disease

Linda S. May-Zhang¹, Zhongyi Chen¹, Noura S. Dosoky¹ , Patricia G. Yancey², Kelli L. Boyd³, Alyssa H. Hasty⁴, MacRae F. Linton² & Sean S. Davies¹

Obesity increases the risk for cardiometabolic diseases. *N*-acyl phosphatidylethanolamines (NAPEs) are precursors of *N*-acylethanolamides, which are endogenous lipid satiety factors. Incorporating engineered bacteria expressing NAPEs into the gut microbiota retards development of diet induced obesity in wild-type mice. Because NAPEs can also exert anti-inflammatory effects, we hypothesized that administering NAPE-expressing bacteria to low-density lipoprotein receptor (*Ldlr*)^{-/-} mice fed a Western diet would improve various indices of cardiometabolic disease manifested by these mice. NAPE-expressing *E. coli* Nissle 1917 (*pNAPE-EcN*), control *Nissle* 1917 (*pEcN*), or vehicle (*veh*) were given via drinking water to *Ldlr*^{-/-} mice for 12 weeks. Compared to *pEcN* or *veh* treatment, *pNAPE-EcN* significantly reduced body weight and adiposity, hepatic triglycerides, fatty acid synthesis genes, and increased expression of fatty acid oxidation genes. *pNAPE-EcN* also significantly reduced markers for hepatic inflammation and early signs of fibrotic development. Serum cholesterol was reduced with *pNAPE-EcN*, but atherosclerotic lesion size showed only a non-significant trend for reduction. However, *pNAPE-EcN* treatment reduced lesion necrosis by 69% indicating an effect on preventing macrophage inflammatory death. Our results suggest that incorporation of NAPE expressing bacteria into the gut microbiota can potentially serve as an adjuvant therapy to retard development of cardiometabolic disease.

Obesity frequently associates with adverse physiological changes including hypertension, hypertriglyceridemia, hypercholesterolemia, and insulin resistance. These changes, commonly termed metabolic syndrome, increase the risks for atherosclerosis, type 2 diabetes, and non-alcoholic fatty liver disease (NAFLD). The rapid rise in obesity in the Western world threatens the decline in mortality from atherosclerosis, the leading cause of death worldwide¹, which have occurred in the past two decades due to cholesterol-lowering drugs such as statins². Dysregulated lipid metabolism accompanied by chronic inflammation is central to the development of atherosclerotic plaques. Subsequent formation of necrotic cores and rupture of these vulnerable atherosclerotic plaques are thought to be critical steps leading to thrombosis, myocardial infarction, and death. The rise in obesity has also markedly increased the prevalence of type 2 diabetes and led to NAFLD becoming the most common cause

¹Division of Clinical Pharmacology, Department of Pharmacology, 2220 Pierce Avenue, Vanderbilt University, 556 Robison Research Building, Nashville, TN, 37221, USA. ²Department of Medicine, Division of Cardiovascular Medicine, Vanderbilt Medical Center, 2220 Pierce Avenue, 312 Preston Research Building, Nashville, TN, 37232, USA. ³AA-6206 Medical Center North, Department of Pathology, Microbiology, and Immunology, Vanderbilt Medical Center, 1211 Medical Center Drive, Nashville, TN, 37232, USA. ⁴Department of Molecular Physiology and Biophysics, Vanderbilt University, 2220 Pierce Avenue, 813 Light Hall, Nashville, TN, 37232, USA. Correspondence and requests for materials should be addressed to S.S.D. (email: sean.davies@vanderbilt.edu)

of abnormal liver function, with 38% of adults in the United States affected³. While early stages of NAFLD are considered relatively benign by clinicians, progression to chronic liver inflammation (non-alcoholic steatohepatitis, NASH), fibrosis, and cirrhosis significantly impacts functionality and lifespan.

One novel therapeutic target for slowing development of metabolic syndrome and cardiometabolic disease is the gut microbiota, as the composition and functionality of the gut microbiota differs in individuals with obesity^{4–7}, atherosclerosis⁸, type 2 diabetes^{9,10}, and/or NAFLD¹¹ compared to their healthy counterparts. Because the gut microbiota chronically releases metabolites that affect various host cells, small but sustained changes in bacterial metabolites can significantly impact disease progression. Recently, we engineered a commensal *E. coli* strain (*Nissle 1917*) to produce *N*-phosphatidylethanolamines (NAPEs), and demonstrated that incorporating these therapeutically modified bacteria (*pNAPE-EcN*) into the gut microbiota retarded the development of obesity and glucose intolerance in wildtype mice fed a high fat diet¹². NAPEs are endogenous anorexigenic lipids normally synthesized by enterocytes of the small intestine (primarily in the duodenum and jejunum) in response to feeding^{13–15}. However, a diet chronically high in fat impairs this intestinal biosynthesis of NAPEs^{16–18}. The mechanisms underlying this impaired biosynthesis are unknown. We reasoned that bacterially-synthesized NAPEs could be used to compensate for this reduced NAPE synthesis. Interestingly, incorporation of NAPE expressing bacteria into the microbiota of the gut (primarily in the large intestine) proved more potent and efficacious than oral administration of purified NAPE¹⁹.

While administration of NAPEs is sufficient to exert therapeutic effects¹⁶, NAPEs undergo hydrolysis to *N*-acyl-ethanolamides (NAEs) by NAPE-hydrolyzing phospholipase D (NAPE-PLD). We found that the anti-obesity effects of our engineered bacteria require NAPE-PLD¹⁹, which supports the notion that NAPEs serve as precursors for NAEs rather than exerting effects directly. NAEs such as C18:1NAE (*N*-oleoylethanolamide) are ligands for receptors including PPAR α , GPR119, and TRPV1. C18:1NAE reduces food intake and increases in fatty acid oxidation, leading to reduced serum triglycerides, and these effects are blunted in PPAR α ^{-/-} mice²⁰. Activation of PPAR α by various agonists induces ApoA1 expression²¹ and increase HDL levels *in vivo*²². C18:1NAE also stimulates GLP-1 release via GPR119 and activation of GPR119 promotes glucose-stimulated insulin secretion²³. GPR119 activation also promotes ABCA1 expression in macrophages and therefore promotes ABCA1-mediated cholesterol efflux by HDL from macrophages²⁴. NAEs also exert direct anti-inflammatory effects^{25–35}. Based on these various effects, increasing NAPE and NAE levels would be anticipated to protect against metabolic syndrome and cardiovascular disease, and in fact, intraperitoneal injection of NAEs in mice can reduce steatosis³⁶, lower LDL levels³⁷, and reduce atherosclerosis^{38,39}.

We hypothesized that administration of NAPE expressing bacteria might be a sustainable, long-term intervention to retard the progression of metabolic syndrome and cardiometabolic disease. To test this hypothesis, we used low density lipoprotein receptor null mice (*Ldlr*^{-/-}), as these mice manifest a number of key aspects of cardiometabolic disease when fed the Western diet. For instance, while feeding a Western diet to wild-type mice induces adiposity, glucose intolerance, and hepatosteatosis, it fails to initiate significant hepatic inflammation or atherosclerosis⁴⁰. In contrast, feeding the Western diet (but not a low fat diet) to *Ldlr*^{-/-} mice initiates steatohepatitis (NASH)^{41–43} and atherosclerosis^{38,44,45}. We examined the effects of administering *pNAPE-EcN* on the development of various indices of cardiometabolic disease in these *Ldlr*^{-/-} mice, and found significant improvements not only in adiposity, but also in reduced hepatic triglycerides, reduced hepatic inflammation and macrophage infiltration, and reduced necrosis of atherosclerotic lesions.

Results

***pNAPE-EcN* reduces body weight and adiposity gain independent of food intake.** Previously, we showed that administration of a probiotic strain of *E. coli*, *Nissle 1917* (*EcN*) transformed with a plasmid for expression of *A. thaliana* NAPE synthase Atlg78690 (*pNAPE-EcN*) in drinking water inhibited development of obesity in C57BL/6J wildtype mice fed a high-fat diet¹². Similar to C57BL6 mice, *Ldlr*^{-/-} mice treated with *pNAPE-EcN* gained relatively less body weight (Fig. 1A) (versus *Veh* 2 weeks, $P < 0.05$; versus *pEcN* 3.5 weeks, $P < 0.05$) and accumulated relatively less body fat (Fig. 1B) (versus *Veh* 4 weeks, $P < 0.05$; versus *pEcN* 8 weeks, $P < 0.05$) compared to vehicle treated mice fed the Western diet during the 12 week treatment period. *pNAPE-EcN* treatment had no effect on food intake (Fig. 1C). Raw values for change in body weight and fat mass are depicted in Supplementary Fig. 1. Furthermore, *pNAPE-EcN* treated animals had lower fasting blood glucose levels than *Veh* treated (153.6 ± 6.9 vs 189.7 ± 6.4 mg/ml, $P < 0.05$) at levels similar to mice fed LFD (149.7 ± 7.0 mg/dl) at 8 weeks (Supplementary Fig. 2).

***pNAPE-EcN* increases hepatic and adipose NAEs.** Bacterial NAPEs absorbed by the intestinal tract are converted into NAEs by NAPE-PLD, resulting in increased levels in liver and adipose tissue^{12,19}. The most prominent NAE species detected in liver of all groups was C18:0NAE and mice fed the Western diet had markedly reduced hepatic NAE levels compared to those fed LFD (Fig. 2). Treatment with *pNAPE-EcN* significantly increased ($P < 0.05$) C18:0NAE levels compared to vehicle treated mice, although these levels were still less than the LFD fed group. The Western diet also markedly reduced NAE levels in adipose tissue compared to LFD, and again treatment with *pNAPE-EcN* treatment increased C18:0NAE levels compared to vehicle treated mice (Fig. 2). Taken together these data suggest that the Western diet markedly reduces endogenous NAE biosynthesis, which is consistent with previous studies in wild-type mice using high fat diets^{16–18}, and that *pNAPE-EcN* treatment partially compensates for this loss.

***pNAPE-EcN* inhibits the accumulation of liver TG and reduces hepatic inflammation and fibrosis.** In contrast to wildtype mice, *Ldlr*^{-/-} mice on a Western diet manifest hepatic inflammation and early fibrosis that mark the progression from simple steatosis towards NASH. We therefore sought to determine the effect of *pNAPE-EcN* on this progression. Hepatosteatosis manifests as a highly vacuolated liver. Animals fed a

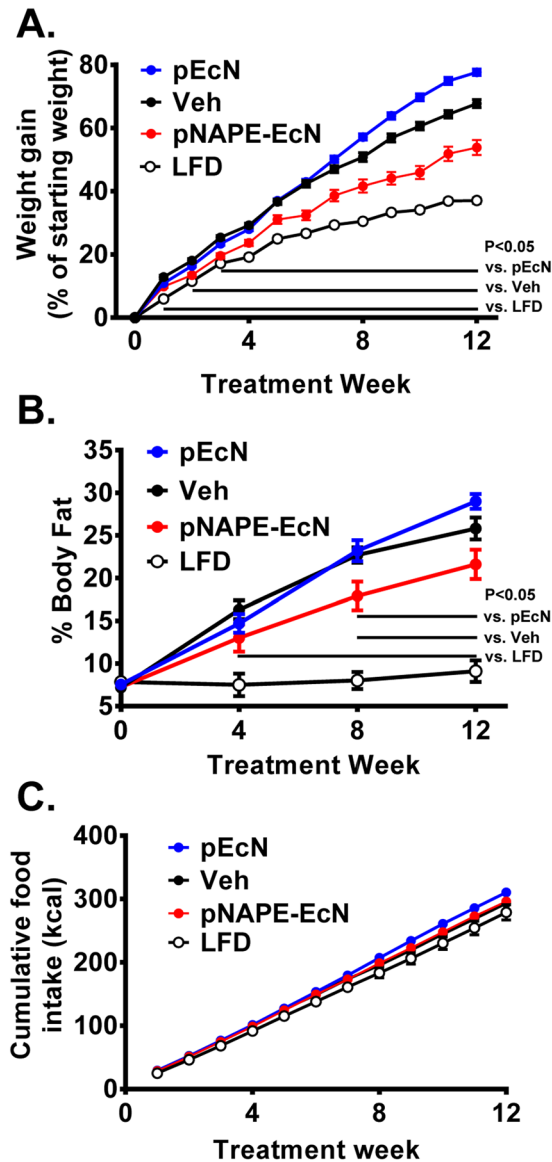


Figure 1. *pNAPE-EcN*, but not *pEcN*, inhibits gain in body weight and adiposity, independent of food intake. All values are mean \pm SEM ($n = 10$ mice per group). *pEcN*, Veh, and *pNAPE-EcN* groups were fed WD for 12 weeks and compared to LFD as an additional control group. (A) Effect on % gain of body weight from start of treatment. (B) Effect on % body fat. (C) Effects on cumulative food intake by energy. Solid bars indicate time points with significant differences ($P < 0.05$) between *pNAPE-EcN* and other groups (2-way repeated measures ANOVA with Dunnett's multiple comparison test). In addition to these differences relative to *pNAPE-EcN*, *pEcN* differed vs Veh $P < 0.05$ starting at 8 weeks for % gain of body weight. LFD differed vs all WD groups $P < 0.05$ starting at 1 week for % gain of body weight and at 4 weeks for % body fat.

Western diet and treated with *vehicle* and *pEcN* displayed multiple hallmarks of hepatosteatosis including markedly elevated hepatic TG levels (Fig. 3A) and highly vacuolated morphology with lipid accumulation (Fig. 3B) compared to animals fed LFD. In contrast, mice treated with *pNAPE-EcN* showed marked reductions in hepatic TG levels (Fig. 3A) ($P < 0.05$ vs. Veh; $P < 0.01$ vs. *pEcN*), improved hepatic morphology, and less lipid accumulation (Fig. 3B). *pNAPE-EcN* treatment reduced hepatic expression of fatty acid transporter *Cd36* (versus *pEcN*, $P < 0.05$) as well as fatty acid synthesis gene *acetyl-CoA carboxylase 1 (Acc1)* (versus Veh, $P < 0.05$) and tended to reduce *Acc2* (versus *pEcN*, $P = 0.06$) (Fig. 3C). *pNAPE-EcN* treatment increased the hepatic expression of genes involved in fatty acid oxidation, *acyl-coA oxidase (Aco)* (versus Veh, $P < 0.01$; versus *pEcN*, $P < 0.001$) and *carnitine acyltransferase 1a (Cpt1a)* (versus *pEcN*, $P < 0.01$) (Fig. 3C). Hepatic expression of *peroxisome proliferator-activated receptors (Ppar α , Ppar δ , Ppar γ)* and *lipoprotein lipase (Lpl)* were not different among any of the groups fed the Western diet (Supplementary Table 2).

pNAPE-EcN treatment reduced molecular markers of diet-induced hepatic inflammation, as indicated in reduced hepatic mRNA expression for genes linked to monocyte and macrophage infiltration (Fig. 4A) such as *C-C motif ligand 2 (Ccl2)*, also known as *monocyte chemoattractant protein 1* or *Mcp1*, *C-C chemokine receptor*

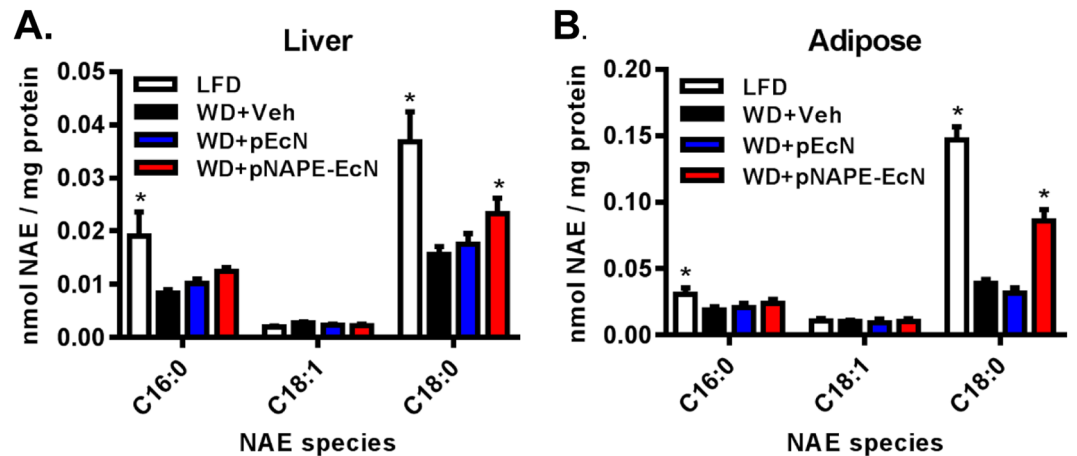


Figure 2. *pNAPE-EcN* increased hepatic and adipose NAE levels at the end of the 12-week study. Values are represented as mean \pm SEM. Statistical significance is * $P < 0.05$ by 2-way ANOVA with Dunnett's multiple comparisons test and denotes comparing to Western diet + *Veh*.

type 2 (*Ccr2*, the receptor for CCL2), and *C-C motif ligand 3* (*Ccl3*, also known as *macrophage inflammatory protein 1-alpha* or *Mip1a*) compared to animals treated with *pEcN*. The expression of both *tumor necrosis factor* (*Tnf α*), and *EGF-like module-containing mucin-like hormone receptor-like 1* (*Emr1*, also known as *F4/80*) was significantly reduced with *pNAPE-EcN* treatment, while the expression of *Integrin subunit alpha M* (*Itgam*, also known as *Cd11b*) only tended to be reduced. Immunostaining for infiltrating monocytes/macrophages using antibodies against *F4/80* revealed that the livers of control mice have large numbers of immunoreactive cells, while *pNAPE-EcN* treated mice had markedly fewer immunoreactive cells (versus *pEcN*, $P < 0.01$) (Fig. 4B,C). Hepatic expression of *Il-6* and *Cd68* were unchanged among any of the groups fed the Western diet (Supplemental Table 2). *pEcN* increased *Il-10* expression compared to both vehicle-treated ($P < 0.001$) and *pNAPE-EcN*-treated groups ($P < 0.001$) (Supplemental Table 2). Taken together, our data show that *pNAPE-EcN* markedly reduces diet-induced hepatic inflammation.

Cytochemical staining with Trichrome Blue revealed only modest fibrosis even in the control *Ldlr*^{-/-} mice fed the Western diet (Fig. 5A), with some mild fibrosis observed around vessels and in sinusoids of *pEcN* treated mice. Despite this lack of visually observable fibrosis, molecular markers indicating the initiation of fibrosis were elevated in vehicle treated mice and suppressed in *pNAPE-EcN* treated mice. For instance, increased mRNA levels of *alpha-smooth muscle actin* (*Sma*)^{46,47} and *tissue inhibitor of metalloproteinases-1* (*Timp1*)⁴⁸ are both early indicators for progression towards hepatic fibrosis. Hepatic expression of *Sma* increased in mice fed a Western diet and treated with either vehicle or control ($P < 0.05$), while mice treated with *pNAPE-EcN* had *Sma* levels similar to the LFD group (Fig. 5B). Mice treated with *pNAPE-EcN* also had reduced hepatic gene expression of *Timp1* (Fig. 5B). Hepatic expression of *transforming growth factor β* (*Tgf β*) was unchanged among groups (Supplemental Table 2). Taken together, the data suggest that *pNAPE-EcN* treatment slowed initiation of hepatic fibrosis.

***pNAPE-EcN* reduces atherosclerotic lesion necrosis.** In humans, lack of functional LDLR markedly increases plasma cholesterol and atherosclerosis, leading to necrotic plaques vulnerable to rupture and which causes thrombosis, vessel occlusion, and myocardial infarctions. *Ldlr*^{-/-} mice on a Western diet have markedly elevated plasma cholesterol levels and their atherosclerotic plaques progress to the early stages of necrosis. We determined the effect of *pNAPE-EcN* treatment on atherosclerotic lesion size and progression in these mice. Treatment with *pNAPE-EcN* reduced plasma cholesterol levels of mice fed a Western diet, compared with those treated with vehicle or *pEcN* (Fig. 6A). Oil Red O staining of proximal aortic sections showed a non-significant trend for a reduction in atherosclerotic lesion size for *pNAPE-EcN* treated mice compared to *vehicle* or *pEcN* (Fig. 6B,C). Similarly, *pNAPE-EcN* caused a non-significant trend for a reduction in atherosclerotic lesion area as examined by *en face* analysis of Sudan IV stained aortas (Fig. 6D,E). Despite the lack of significant changes in aortic lesion size, *pNAPE-EcN* treatment markedly decreased the necrotic area within the atherosclerotic lesion quantified by H&E staining by 69% (Fig. 7A,B) ($P < 0.001$). Lesional collagen content tended to be increased with *pNAPE-EcN* treatment compared to *vehicle* or *pEcN* but the difference was not statistically significant (Fig. 7C,D). These results suggest that while the modest reduction in cholesterol levels induced by *pNAPE-EcN* did not significantly impact atherosclerotic lesion development, the anti-inflammatory effects of NAEs prevented the formation of more vulnerable necrotic plaques.

Discussion

Ldlr^{-/-} mice fed a Western diet manifest a number of key features of human cardiometabolic disease and show a marked diminution in tissue NAE levels, so they represent an important model for determining the potential of NAE expressing bacteria to treat human disease. Our finding that feeding the Western diet reduced liver and adipose NAE levels in these mice is consistent with previous studies showing that high fat diets reduced NAE and NAE levels, at least in the small intestine^{16–18}. The mechanisms of this diet induced reduction in biosynthesis is not known and warrants further study. However, that this reduction may have important implications for

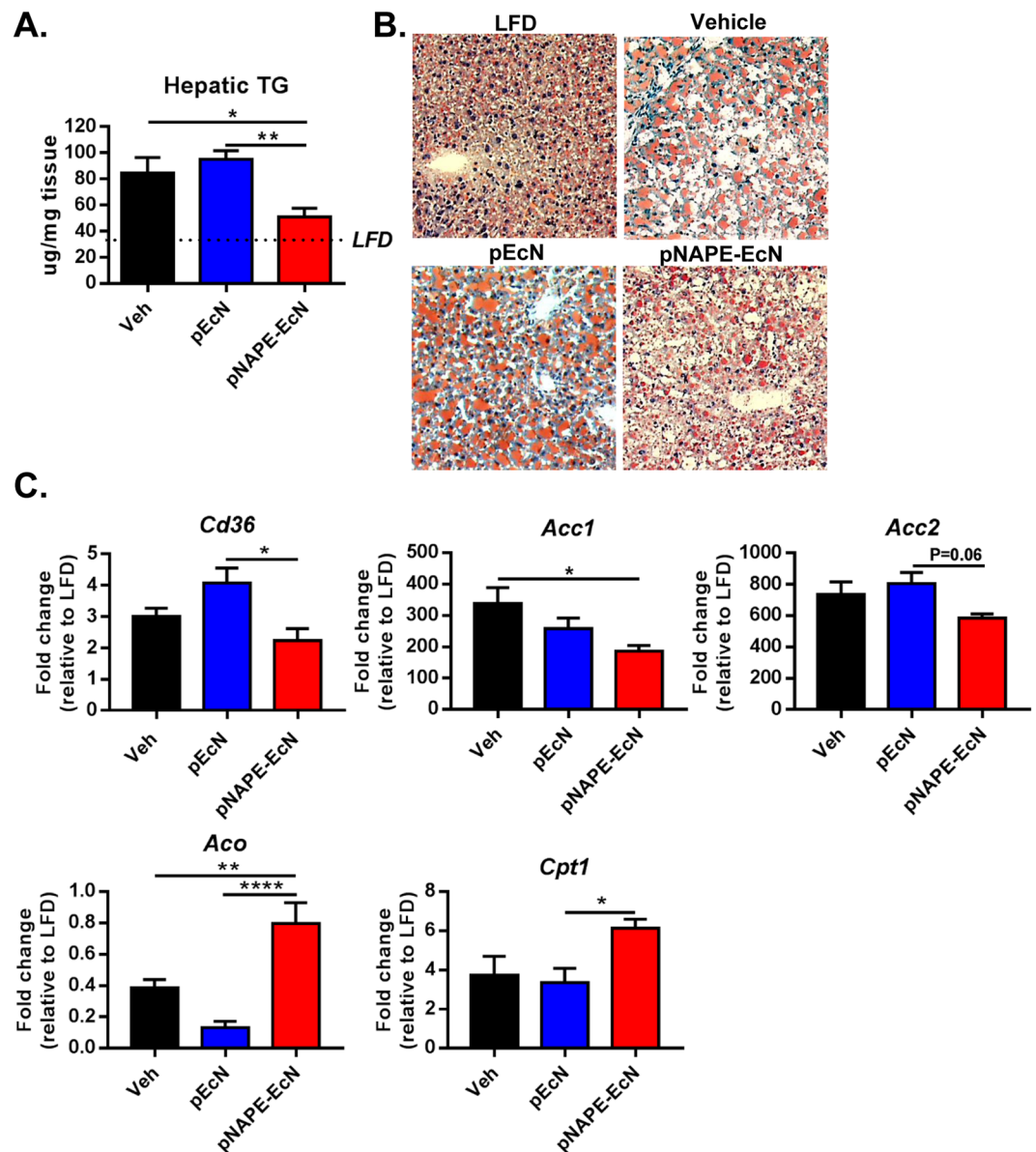


Figure 3. *pNAPE-EcN* reduces development of diet-induced hepatosteatosis. (A) Effect of treatments ($n = 9-10$ animals per group) on hepatic TG levels at the end of the 12-week study. (B) Representative images of liver sections stained with Oil Red O. (C) Effect of treatments on hepatic mRNA expression of *Cd36*, *Acc1*, *Acc2*, *Aco*, and *Cpt1a*. Values are represented as mean \pm SEM. Dotted line represents animals on low fat diet as a comparison. Statistical significance is $*P < 0.05$; $**P < 0.01$; $****P < 0.001$ by 1-way ANOVA with Dunnett's multiple comparisons test.

cardiometabolic disease is shown by our findings that treatment of *Ldlr*^{-/-} mice with *pNAPE-EcN* was able to partially restore tissue NAE levels and markedly reduced a number of key markers of cardiometabolic disease in these mice, such as hepatosteatosis, inflammation, and the formation of necrotic atherosclerotic plaques. Thus, incorporating NAPE expressing bacteria into the gut microbiota has potential as an adjuvant therapy to slow the progression of cardiometabolic disease. These studies extend our previous findings showing that incorporating NAPE expressing bacteria into the gut microbiota slowed the development of obesity, glucose intolerance, and insulin resistance in wildtype C57BL/6 mouse fed a high fat diet.

Although previous studies indicated that administration of NA(P)Es protect against obesity and hepatosteatosis^{12,36}, our findings with *Ldlr*^{-/-} mice provide additional insights into the mechanisms whereby NA(P)Es exert protective effects in the liver. *pNAPE-EcN* did not alter food intake in the *Ldlr*^{-/-} mice, in contrast to wild-type mice fed a high-fat diet where reduced food intake significantly contributed to the reduced hepatosteatosis induced by *pNAPE-EcN*¹². The mechanism underlying the loss of this anorexic effect of *pNAPE-EcN* in *Ldlr*^{-/-} mice is not clear, but previous studies have demonstrated that activation of PPAR α induces *Ldlr* expression⁴⁹. Since the loss of *Ldlr* has previously been shown to alter feeding behavior and sensitivity to leptin under some

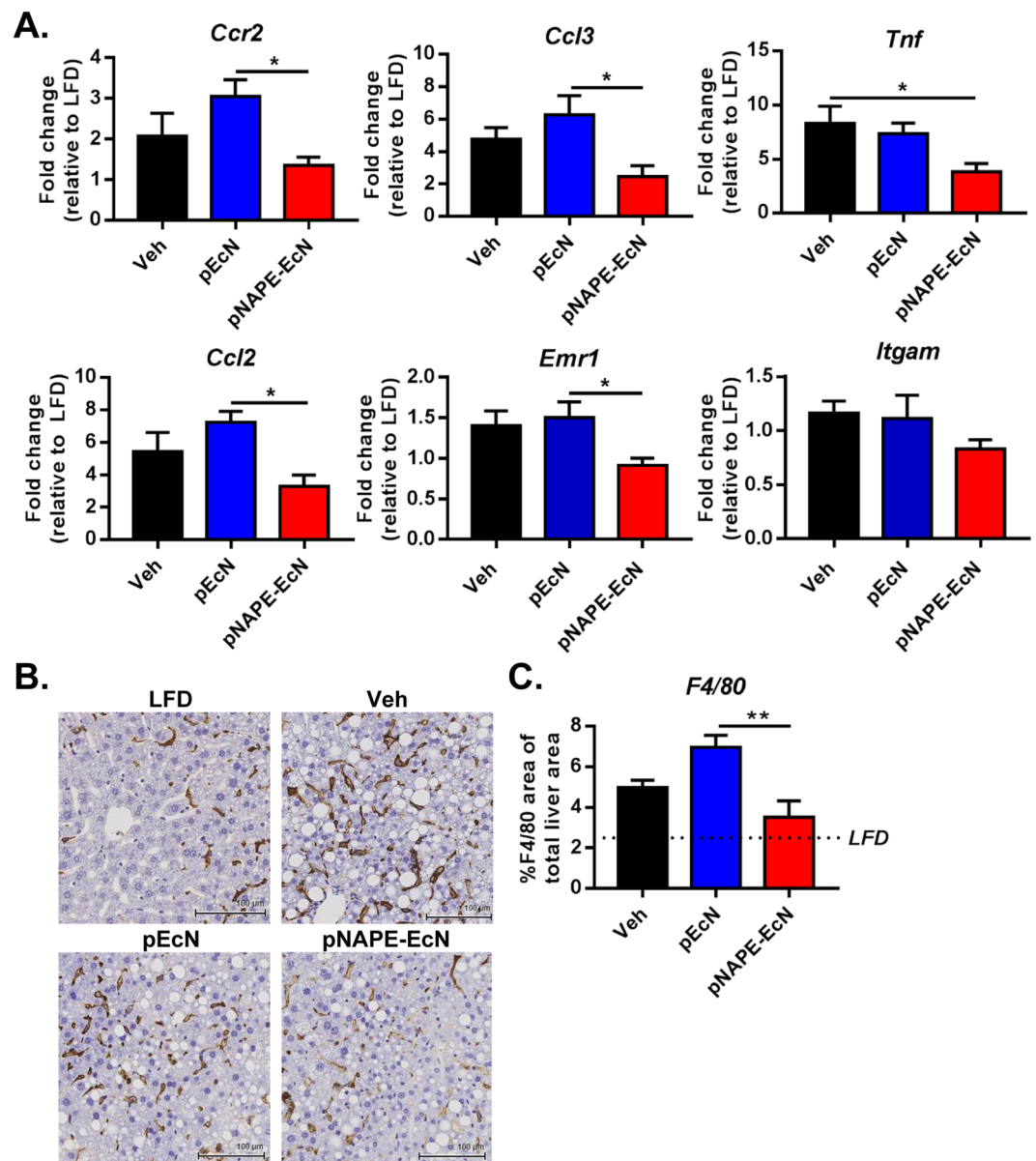


Figure 4. *pNAPE-EcN* reduces diet-induced hepatic inflammation. **(A)** Effect of treatments on expression of hepatic genes involved in inflammation and macrophage infiltration at the end of the 12-week study. Values are represented as mean \pm SEM. Dotted lines represent animals on a low fat diet. Statistical significance is * $P < 0.05$ by 1-way ANOVA with Dunnett's multiple comparisons test. **(B)** Representative images of liver sections immunostained for F4/80. **(C)** Digital quantitation of F4/80-stained slides expressed as % F4/80-stained area of total liver area.

conditions⁵⁰, we speculate that the NAPE/NAE/PPAR α pathways leading to reduced food intake in wild-type mice is dependent in some way on functional LDLR. Future studies are needed to elucidate this relationship.

In the *Ldlr*^{-/-} mice, clearly other mechanisms besides a reduction in food intake must drive the reduced body weight gain and hepatic fat accumulation. Although we did not measure energy expenditure and resting metabolic rate in these experiments, our previous studies suggest that these could be key mechanisms. In wild-type mice, treatment with *pNAPE-EcN* increased resting metabolic rate (but not physical activity) in addition to reducing food intake, and increased expression of fatty acid oxidation genes such as *Aco* seemed to underlie the increased resting metabolic rate. In the *Ldlr*^{-/-} mice, treatment with *pNAPE-EcN* also increased expression of *Aco* and *Cpt1a*, as well as decreased hepatic expression of *Cd36*, *Acc1*, and *Acc2*. Therefore, we speculate that *Ldlr*^{-/-} mice treated with *pNAPE-EcN* may also have increased resting metabolic rates which would then account for their reduced adiposity despite no change in food intake.

Previous studies suggest that such changes can protect against hepatosteatosis. CD36 serves as a transporter of long chain fatty acids and as a receptor for these ligands that trigger phospholipase C activity and calcium signaling⁵¹. Liver specific deletion of *Cd36* in mice fed a high fat diet markedly reduces hepatic accumulation of TG and

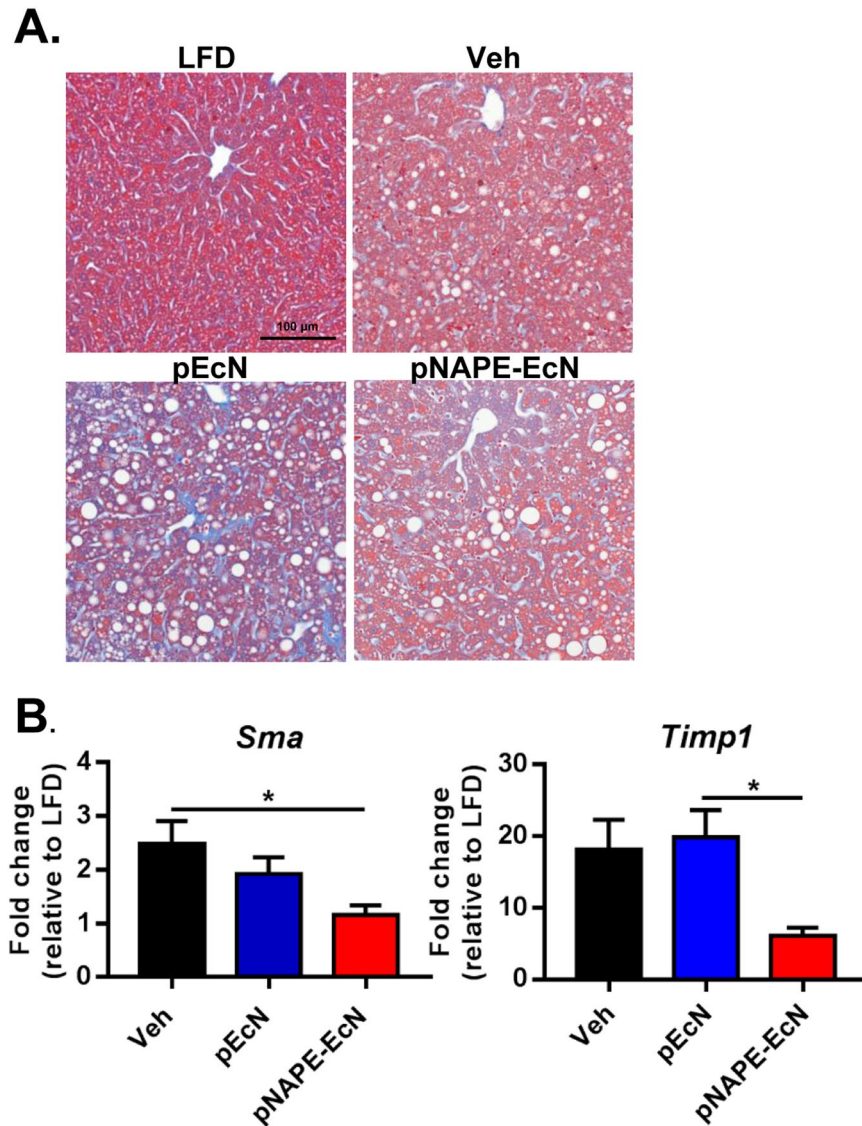


Figure 5. *pNAPE-EcN* reduces initiation of hepatic fibrosis. **(A)** Representative images of Trichrome Blue staining of liver sections. **(B)** Effects of treatment on hepatic gene expression of smooth muscle actin and tissue inhibitor of metalloproteinase 1 at the end of the 12-week study. Values are represented as mean \pm SEM. Dotted lines represent animals on a low fat diet. Statistical significance is * $P < 0.05$ by 1-way ANOVA with Dunnett's multiple comparisons test.

expression of inflammatory markers⁵². In human patients undergoing bariatric surgery for morbid obesity, the extent of hepatic *CD36* downregulation after bariatric surgery correlates with improvements in steatosis⁵³. *Acc1* is the rate-limiting step for de novo lipogenesis whereas *Acc2* generates malonyl-CoA to allosterically inhibit *Cpt1*⁵⁴. Liver-specific knockout of *Acc1* in mice protects against hepatic steatosis^{55,56}, and pharmacological inhibition of *Acc* reduces de novo lipogenesis, enhances fatty acid oxidation, and reduces hepatic TG in preclinical and human studies⁵⁷. *Aco* catalyzes β -oxidation of very long chain fatty acids, and mice lacking *Aco* develop severe microvesicular steatohepatitis^{58,59}. *Cpt1* is a mitochondrial enzyme that transfers fatty acids from the cytosol prior to β -oxidation, with *Cpt1a* being the hepatic isoform. *CPT1* expression is reduced in humans by 50% in NAFLD compared to normal subjects⁶⁰. Therefore, increased expression of *Aco* and *Cpt1a* in *pNAPE-EcN* treated mice is consistent with protection against hepatosteatosis.

Treatment with *pNAPE-EcN* not only altered expression of fat metabolizing genes, but reduced expression of genes associated with inflammation including *Tnf α* , *Ccl2*, and *F4/80*. These changes are consistent with previous reports of anti-inflammatory effects of NAEs. For instance, C16:0NAE (*N*-palmitoylethanolamide) inhibits a wide variety of inflammatory activities including mast cell activation^{25,26}; pattern recognition molecule induction of eicosanoids and cytokines and leukocyte infiltration^{27–31}; ischemia-reperfusion injury³²; dextran sodium sulfate induced colitis and enteric glial cell activation⁶¹; and diabetic retinopathy³³. Both C18:1NAE and C18:0NAE have also been reported to exhibit anti-inflammatory effects^{34,35}. In addition to the expression of inflammatory genes, initiation of the fibrotic response is another important step in the development of steatohepatitis. Although

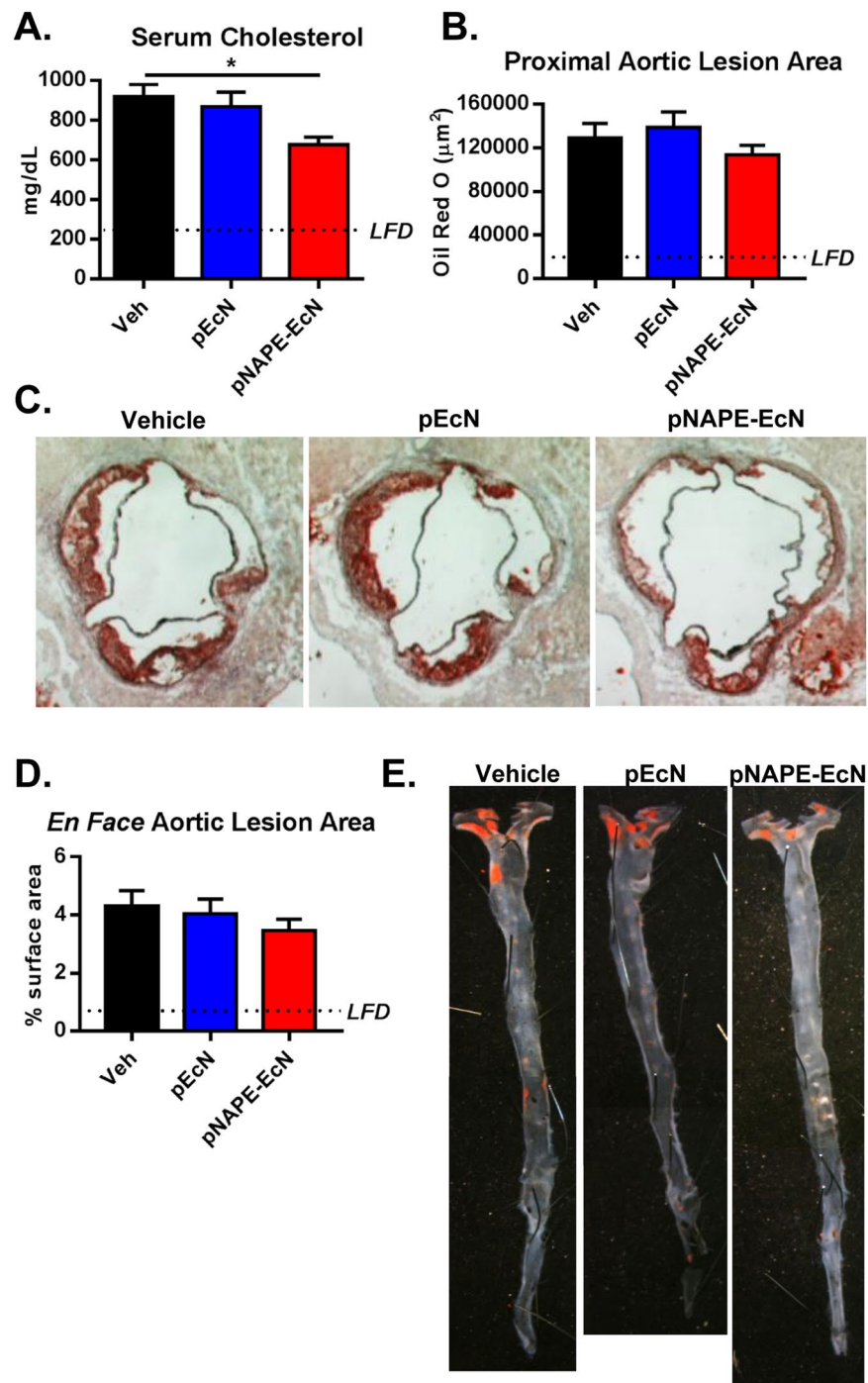


Figure 6. Effects of *pNAPE-EcN* on serum cholesterol levels and atherosclerotic lesion size at the end of the 12-week study. **(A)** Serum total cholesterol levels were determined by enzymatic methods. Absorbance was measured at 500 nm. **(B)** Effect of treatments on proximal aortic lesion area as determined by Oil Red O staining. **(C)** Representative images of Oil Red O stained proximal aortic sections. **(D)** Effect of treatments on atherosclerosis determined by en face analysis of Sudan IV stained aortas. **(E)** Representative images of Sudan IV stained aortas. Dotted lines represent animals on a low fat diet. Values are represented as mean \pm SEM. * $P < 0.05$. Statistical significance by 1-way ANOVA with Dunnett's multiple comparisons test.

fibrosis was not visually observable in vehicle-treated *Ldlr*^{-/-} mice after 12 weeks of the Western diet, *Sma* and *Timp1* are both important molecular indicators that the fibrotic response has been initiated^{46–48}, and their expression was elevated. Treatment with *pNAPE-EcN* suppressed their expression, suggesting that NAEs can also block the initiation of fibrosis. Together, our findings suggest that treatment with *pNAPE-EcN* has the potential to retard development of NASH in humans exposed to obesogenic diets.

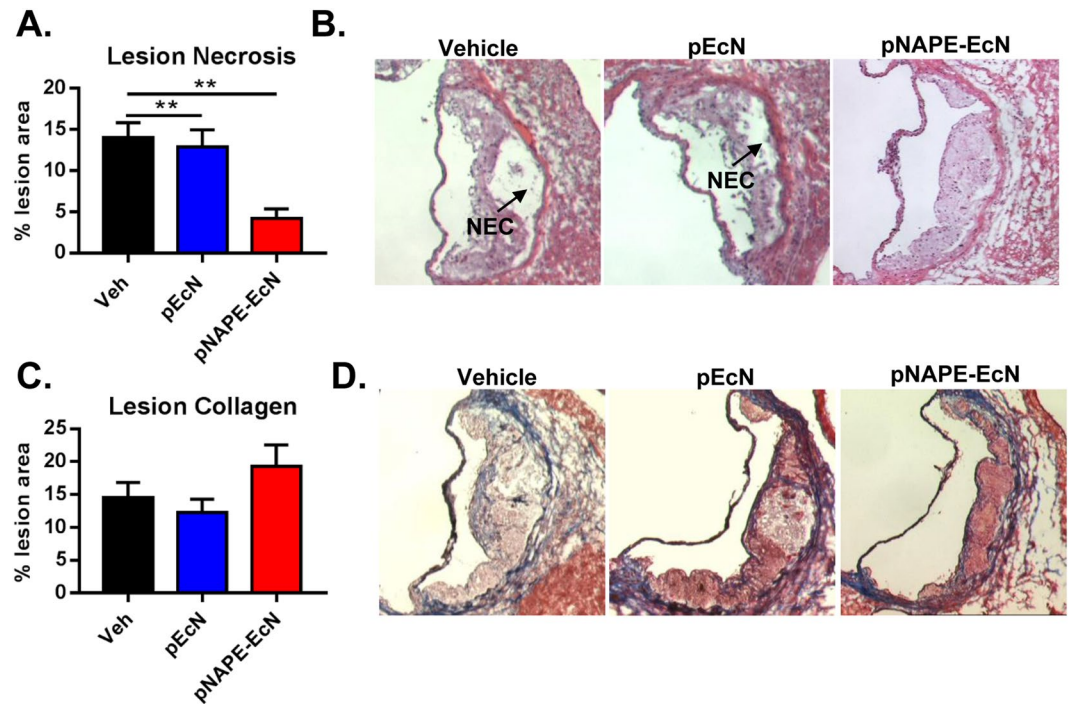


Figure 7. Effects of *pNAPE-EcN* on lesion necrosis and collagen at the end of the 12-week study. (A) Effect of treatments ($n = 8$ animals per group) on cross-sectional necrotic area (NEC) determined by a lack of H&E staining in the lesion area. (B) Representative images of H&E stained slides. (C) Effect of treatments on lesion collagen content determined by Trichrome Blue. (D) Representative images of Trichrome blue staining. Values are represented as mean \pm SEM.

In regards to cardiovascular disease, the most important findings of our study were that *pNAPE-EcN* reduced plasma cholesterol levels and necrosis in atherosclerotic lesions in the *Ldlr*^{-/-} mice. Our finding of reduced cholesterol levels concurs with a previous report that administration of C18:1NAE (10 mg/kg/day i.p.) for 8 weeks to *ApoE*^{-/-} mice fed a Western diet lowered total and LDL cholesterol levels compared to vehicle treated mice³⁷. Although a previous study with C18:1NAE in *ApoE*^{-/-} mice found reduced atherosclerotic lesion area³⁷, we did not find that treatment with *pNAPE-EcN* significantly decreased atherosclerotic lesion size, but rather reduced necrotic area within the atherosclerotic lesion, consistent with an effect on reducing macrophage cell death. The contribution of macrophages to plaque morphology is size-independent and vulnerable plaques are characterized by the formation of the necrotic core and thinning of the fibrous cap. Our finding is particularly significant because lesion area is considered a poor predictor of clinical disease in humans⁶², with more advanced plaque features such as the necrotic core formation considered more important indicators⁶³.

The anti-atherosclerotic effects of *pNAPE-EcN* treatment are consistent with the ability of NAEs to act as agonists of both PPAR α and GPR119. PPAR α agonists induce expression of ApoAI²¹ and decrease ApoC-III production⁶⁴. ApoAI is the major protein component of HDL and facilitates efflux of cholesterol from macrophages via ABCA1, while ApoC-III is primarily a component of VLDL that increases plasma triglycerides by inhibiting lipoprotein lipase. *In vivo*, PPAR α agonists such as fibrates increase HDL levels while modestly reducing LDL cholesterol levels²². In addition to driving cholesterol efflux, ApoAI may protect macrophages against necrosis, as ectopic expression of ApoAI in macrophages that are subsequently transplanted into *Ldlr*^{-/-}; *ApoAI*^{-/-} mice leads to reduced necrotic core area without affecting aortic macrophage levels⁶⁵. Agonism of GPR119 by NAEs may synergize with their effects on PPAR α , as GPR119 activation was recently shown to increase ABCA1 expression in macrophages, and to thereby increase cholesterol efflux from macrophages²⁴. Thus, agonism of both PPAR α and GPR119 may mediate the anti-atherosclerotic effects of *pNAPE-EcN* treatment. Mechanisms underlying the effect of NA(P)Es on advanced plaque features warrant further investigation. Nevertheless, this protection against necrosis suggest the potential value of *pNAPE-EcN* as an adjuvant therapy for treating atherosclerosis, since ruptures of vulnerable plaques lead to occlusive thrombosis, myocardial infarction, and death in humans with cardiovascular disease.

Finally, we note that our strategy of using gut bacteria engineered to produce NAEs offers advantages over two obvious alternative strategies. While altering the gut microbial composition through use of traditional pre- or pro-biotics may be useful^{66,67}, our strategy offers the advantage of sustained delivery of precisely characterized therapeutic compounds using a bacterial strain that reliably colonizes. Alternatively, traditional oral delivery of purified NA(P)Es can also be employed, but we previously found that bacterial biosynthesis of NAE in the intestinal tract was more potent and efficacious than oral administration of purified NAE¹⁹, and that colonization of *pNAPE-EcN* provided protection even weeks after ending administration¹². For these reasons, incorporating *pNAPE-EcN* or other bacteria engineered to express NAE into the gut microbiota appears to have significant potential as a long-term adjuvant strategy for slowing the development of metabolic syndrome and cardiometabolic disease.

Methods

Bacterial strains and preparation. *EcN* (Ardey Pharm, GmbH) was transformed with *pNAPE* (*At1g78690*) as previously described¹². Briefly, for expression of *pNAPE* in *EcN*, *pQE-80L* (QIAGEN) was modified by removing one lac operator to enable a basal expression of inserted genes without isopropyl β -D-1-thiogalactopyranoside induction. The *At1g78690* gene was obtained by high-fidelity PCR using pDEST-*At1g78690*⁶⁸ as a template, and subcloned in frame into *pQE-80L1* digested with BamHI and SacI.

Animal studies. Public Health Services guidelines regarding the use and care of laboratory animals were observed. All procedures involving animals were approved by the Vanderbilt University Institutional Animal Care and Use Committee. Forty male *Ldlr*^{-/-} mice on a C57BL/6J background were purchased at 5 weeks old (Jackson Laboratories, Bar Harbor, ME; stock number 002207) and housed in standard mouse cages with bedding at the Vanderbilt University animal facility in a 12-hour light/12-hour dark cycle, with food and water given *ad libitum*. The animals were acclimated for 1 week and maintained on standard rodent chow (LabDiet 5001). The animals were divided into 4 experimental groups of 10 mice each, and housed individually (1 mouse per cage) to measure food intake. To reduce the gut microbiota prior to bacteria administration, the animals were gavaged with an antibiotic cocktail (10 μ l/g body weight) containing amphotericin B (0.3 mg/ml), metronidazole (10 mg/ml), vancomycin (0.5 mg/ml), neomycin (10 mg/ml), and ampicillin (10 mg/ml) for 3 consecutive days. Three experimental groups were switched to a Western diet (Harlan Laboratories, catalog #TD.10885) containing 45% fat by kcal, while the fourth group was switched to a low fat control diet (LFD) (Harlan Laboratories, Inc, catalog #TD.120724). Groups fed the Western diet (WD) received standard drinking water containing vehicle (0.125% gelatin) as a control, control *Nissle 1917* (*pEcN*) (5×10^9 CFU/ml suspended in 0.125% gelatin), or NAPE-expressing *Nissle 1917* (*pNAPE-EcN*) (5×10^9 CFU/ml suspended in 0.125% gelatin). The chow-fed group received standard drinking water containing vehicle as an additional control group. Fresh drinking water and bacteria preparations were given 3 times a week. The treatments continued for 12 weeks before euthanasia. During this period, body weights and food intake were measured twice weekly. Body composition was measured by nuclear magnetic resonance analyses (Bruker Minispec MQ10). Before the morning of euthanasia, animals were fasted overnight. Under isoflurane anesthesia, blood samples were collected via retro-orbital venous plexus puncture. The animals were then euthanized via isoflurane overdose followed by cervical dislocation. The left ventricle of the heart was flushed with 30 mL saline. Liver and adipose samples were collected as tissues frozen in liquid nitrogen and as samples fixed in neutral buffered formalin for sectioning. The entire aorta was dissected for *en face* preparation as previously described⁴⁵. The heart with the proximal aorta was embedded in optimal cutting temperature compound and frozen on dry ice. Preparation and analyses of tissues are described below.

Hepatic TG and NAPE measurements. For hepatic TG measurements, lipids were extracted using chloroform/methanol (2:1), and individual lipid classes were separated by thin-layer chromatography. The TGs were scraped from the plate, and the fatty acids methylated using BF₃/methanol. Fatty acid methyl esters were analyzed using an Agilent 7890 A gas chromatograph equipped with flame ionization detectors and a capillary column (SP2380, 0.25 mm \times 30 m, 0.25 μ m film; Supelco). The esters were identified by comparing the retention times to those of known standards. Triicosenoin (C20:1) was added to the total lipid extract, serving as an internal standard and permitting quantitation of the amount of TGs in the sample.

Liver staining and immunohistochemistry. For staining and immunohistochemistry procedures, frozen liver cyrosections were prepared at 10 microns thick on microscope slides. For Oil Red O staining, freshly cut liver sections were fixed in neutral buffered formalin before rinsing in water and equilibration in 60% isopropanol. Slides were then stained with Oil Red O (Sigma, Aldrich, St. Louis, MO) working solution prepared in 100% isopropanol. For H&E staining of liver sections, slides were stained with hematoxylin (Richard-Allan), Bluing Reagent (Richard-Allan), and Eosin-Y (Richard-Allan). For Trichrome Blue staining, slides were stained with a Masson's Trichrome stain kit (Dako, North America, Inc). For *F4/80* immunohistochemistry, enzymatic induced antigen retrieval was performed using Proteinase K (Dako, North America, Inc) for 5 minutes. Slides were incubated with anti-*F4/80* (NB600-404, Novus Biologicals) for at a 1:1000 dilution and then incubated in a rabbit anti-rat secondary (BA-4001, Vector Laboratories, Inc.) at a 1:200 dilution. The Bond Polymer Refine detection system was used for visualization. After staining, slides were dehydrated, cleared and coverslipped. Immunostained tissue microarray slides were imaged on a Leica SCN400 Slide Scanner (Leica Biosystems). Tissue cores were imaged at 20X magnification to a resolution of 0.5 μ m/pixel. Cells were identified utilizing standard Ariol analysis scripts. (Leica) Upper and lower thresholds for color, saturation, intensity, size were set for both blue Hematoxylin staining of nuclei and for brown DAB reaction products, so that the brown (DAB) positive cells can be distinguished from blue (Hematoxylin only) negative cells. The area of positive *F4/80* staining area was calculated as a percent of the total analyzed area. $ddc'1 \times$.

Hepatic gene expression. Total RNA was extracted from frozen liver tissue using the RNeasy Micro Kit (QIAGEN), and transcribed into cDNA using a cDNA reverse transcription kit (Applied Biosystems). Gene expression levels were quantified by RT-PCR using SYBR Green PCR Master Mix (QIAGEN) and the 7500 Real Time PCR system (Applied Biosystems). Primer sequences are described in Supplementary Table 1. Relative quantification of gene expression with real-time PCR data was calculated relative to *Ppia* (*cyclophilin*).

Quantification of Arterial Lesions. Cryosections of the proximal aorta that were 10 microns thick were prepared starting at the aortic sinus and continuing 300 microns distally on microscope slides, according to the method of Paigen *et al.*⁶⁹ and adapted for computer analysis⁷⁰. Sections were stained with Oil Red O and counterstained with hematoxylin. Additional slides were stained with H&E and Trichrome as described above. *En face*

aortas were stained with Sudan IV solution (Sigma-Aldrich). The images of the aorta were captured and analyzed with an imaging system (KS 300 Release 2.0; Kontron Elektronik GmbH).

Serum Cholesterol. Serum concentrations of total cholesterol were determined by enzymatic methods (Raichem) according to the manufacturer's instructions. Absorbance was measured at 500 nm.

Statistical Analysis. Statistical analysis was performed using GraphPad Prism 7. A *P* value of less than 0.05 was considered statistically significant. For 2-way repeated-measures ANOVA, when overall significance for treatment effect was found, the Bonferroni's multiple comparison post-hoc test was used to determine differences between treatment groups. For 1-way ANOVA, when overall significance for treatment effect was found, the Dunnett's multiple comparison post-hoc test was used to determine groups that differed from the control group.

Data Availability Statement

The datasets generated during the current study are available from the corresponding author on reasonable request.

References

- Weber, C. & Noels, H. Atherosclerosis: current pathogenesis and therapeutic options. *Nat Med* **17**, 1410–1422, <https://doi.org/10.1038/nm.2538> (2011).
- Herrington, W., Lacey, B., Sherliker, P., Armitage, J. & Lewington, S. Epidemiology of Atherosclerosis and the Potential to Reduce the Global Burden of Atherothrombotic Disease. *Circ Res* **118**, 535–546, <https://doi.org/10.1161/CIRCRESAHA.115.307611> (2016).
- Anstee, Q. M., Targher, G. & Day, C. P. Progression of NAFLD to diabetes mellitus, cardiovascular disease or cirrhosis. *Nat Rev Gastroenterol Hepatol* **10**, 330–344, <https://doi.org/10.1038/nrgastro.2013.41> (2013).
- Ley, R. E., Turnbaugh, P. J., Klein, S. & Gordon, J. I. Microbial ecology: human gut microbes associated with obesity. *Nature* **444**, 1022–1023, <https://doi.org/10.1038/4441022a> (2006).
- Zhang, H. *et al.* Human gut microbiota in obesity and after gastric bypass. *Proc Natl Acad Sci USA* **106**, 2365–2370, <https://doi.org/10.1073/pnas.0812600106> (2009).
- Armougom, F., Henry, M., Vialettes, B., Raccach, D. & Raoult, D. Monitoring bacterial community of human gut microbiota reveals an increase in *Lactobacillus* in obese patients and *Methanogens* in anorexic patients. *PLoS One* **4**, e7125, <https://doi.org/10.1371/journal.pone.0007125> (2009).
- Schwartz, A. *et al.* Microbiota and SCFA in lean and overweight healthy subjects. *Obesity (Silver Spring)* **18**, 190–195, <https://doi.org/10.1038/oby.2009.167> (2010).
- Wang, Z. *et al.* Gut flora metabolism of phosphatidylcholine promotes cardiovascular disease. *Nature* **472**, 57–63, <https://doi.org/10.1038/nature09922> (2011).
- Larsen, N. *et al.* Gut microbiota in human adults with type 2 diabetes differs from non-diabetic adults. *PLoS One* **5**, e9085, <https://doi.org/10.1371/journal.pone.0009085> (2010).
- Qin, J. *et al.* A metagenome-wide association study of gut microbiota in type 2 diabetes. *Nature* **490**, 55–60, <https://doi.org/10.1038/nature11450> (2012).
- Spencer, M. D. *et al.* Association between composition of the human gastrointestinal microbiome and development of fatty liver with choline deficiency. *Gastroenterology* **140**, 976–986, <https://doi.org/10.1053/j.gastro.2010.11.049> (2011).
- Chen, Z. *et al.* Incorporation of therapeutically modified bacteria into gut microbiota inhibits obesity. *J Clin Invest* **124**, 3391–3406, <https://doi.org/10.1172/JCI72517> (2014).
- Fu, J. *et al.* Food intake regulates oleoylethanolamide formation and degradation in the proximal small intestine. *J Biol Chem* **282**, 1518–1528, <https://doi.org/10.1074/jbc.M607809200> (2007).
- Tinoco, A. B. *et al.* Role of oleoylethanolamide as a feeding regulator in goldfish. *The Journal of Experimental Biology* **217**, 2761–2769, <https://doi.org/10.1242/jeb.106161> (2014).
- Astarita, G. *et al.* Postprandial increase of oleoylethanolamide mobilization in small intestine of the Burmese python (*Python molarus*). *Am J Physiol Regul Integr Comp Physiol* **290**, R1407–1412, <https://doi.org/10.1152/ajpregu.00664.2005> (2006).
- Gillum, M. P. *et al.* N-acylphosphatidylethanolamine, a gut-derived circulating factor induced by fat ingestion, inhibits food intake. *Cell* **135**, 813–824, <https://doi.org/10.1016/j.cell.2008.10.043> (2008).
- Diep, T. A. *et al.* Dietary Non-Esterified Oleic Acid Decreases the Jejunal Levels of Anorectic N-Acylethanolamines. *PLoS ONE* **9**, e100365, <https://doi.org/10.1371/journal.pone.0100365> (2014).
- Diep, T. A. *et al.* Dietary fat decreases intestinal levels of the anorectic lipids through a fat sensor. *The FASEB Journal* **25**, 765–774, <https://doi.org/10.1096/fj.10-166595> (2011).
- Chen, Z. *et al.* Leptogenic effects of NAPE require activity of NAPE-hydrolyzing phospholipase D. *J Lipid Res* **58**, 1624–1635, <https://doi.org/10.1194/jlr.M076513> (2017).
- Fu, J. *et al.* Oleoylethanolamide regulates feeding and body weight through activation of the nuclear receptor PPAR- α . *Nature* **425**, 90–93, <https://doi.org/10.1038/nature01921> (2003).
- Singh, J. P. *et al.* Identification of a Novel Selective Peroxisome Proliferator-Activated Receptor α Agonist, 2-Methyl-2-(4-{3-[1-(4-methylbenzyl)-5-oxo-4,5-dihydro-1H-1,2,4-triazol-3-yl]propyl}phenoxy)propanoic Acid (LY518674), That Produces Marked Changes in Serum Lipids and Apolipoprotein A-1 Expression. *Molecular Pharmacology* **68**, 763–768, <https://doi.org/10.1124/mol.105.010991> (2005).
- Staels, B. *et al.* Mechanism of action of fibrates on lipid and lipoprotein metabolism. *Circulation* **98**, 2088–2093 (1998).
- Lauffer, L. M., Iakoubov, R. & Brubaker, P. L. GPR119 is essential for oleoylethanolamide-induced glucagon-like peptide-1 secretion from the intestinal enteroendocrine L-cell. *Diabetes* **58**, 1058–1066, <https://doi.org/10.2337/db08-1237> (2009).
- Hu, Y.-W. *et al.* A lincRNA-DYNLRB2-2/GPR119/GLP-1R/ABCA1-dependent signal transduction pathway is essential for the regulation of cholesterol homeostasis. *Journal of Lipid Research* **55**, 681–697, <https://doi.org/10.1194/jlr.M044669> (2014).
- Facci, L. *et al.* Mast cells express a peripheral cannabinoid receptor with differential sensitivity to anandamide and palmitoylethanolamide. *Proc Natl Acad Sci USA* **92**, 3376–3380 (1995).
- Mazzari, S., Canella, R., Petrelli, L., Marcolongo, G. & Leon, A. N-(2-hydroxyethyl)hexadecanamide is orally active in reducing edema formation and inflammatory hyperalgesia by down-modulating mast cell activation. *Eur J Pharmacol* **300**, 227–236 (1996).
- Berdyshev, E., Boichot, E., Corbel, M., Germain, N. & Lagente, V. Effects of cannabinoid receptor ligands on LPS-induced pulmonary inflammation in mice. *Life Sci* **63**, PL125–129 (1998).
- Costa, B., Conti, S., Giagnoni, G. & Colleoni, M. Therapeutic effect of the endogenous fatty acid amide, palmitoylethanolamide, in rat acute inflammation: inhibition of nitric oxide and cyclo-oxygenase systems. *British journal of pharmacology* **137**, 413–420, <https://doi.org/10.1038/sj.bjp.0704900> (2002).
- Genovese, T. *et al.* Effects of palmitoylethanolamide on signaling pathways implicated in the development of spinal cord injury. *The Journal of pharmacology and experimental therapeutics* **326**, 12–23, <https://doi.org/10.1124/jpet.108.136903> (2008).

30. Solorzano, C. *et al.* Selective N-acylethanolamine-hydrolyzing acid amidase inhibition reveals a key role for endogenous palmitoylethanolamide in inflammation. *Proc Natl Acad Sci USA* **106**, 20966–20971, <https://doi.org/10.1073/pnas.0907417106> (2009).
31. Conti, S., Costa, B., Colleoni, M., Parolaro, D. & Giagnoni, G. Antiinflammatory action of endocannabinoid palmitoylethanolamide and the synthetic cannabinoid nabilone in a model of acute inflammation in the rat. *British journal of pharmacology* **135**, 181–187, <https://doi.org/10.1038/sj.bjp.0704466> (2002).
32. Di Paola, R. *et al.* Effects of palmitoylethanolamide on intestinal injury and inflammation caused by ischemia-reperfusion in mice. *J Leukoc Biol* **91**, 911–920, <https://doi.org/10.1189/jlb.0911485> (2012).
33. Paterniti, I. *et al.* Palmitoylethanolamide treatment reduces retinal inflammation in streptozotocin-induced diabetic rats. *Eur J Pharmacol* **769**, 313–323, <https://doi.org/10.1016/j.ejphar.2015.11.035> (2015).
34. Sayd, A. *et al.* Systemic administration of oleoylethanolamide protects from neuroinflammation and anhedonia induced by LPS in rats. *Int J Neuropsychopharmacol* **18**, <https://doi.org/10.1093/ijnp/pyu111> (2014).
35. Dalle Carbonare, M. *et al.* A Saturated N-Acylethanolamine Other than N-Palmitoyl Ethanolamine with Anti-inflammatory Properties: a Neglected Story. *Journal of Neuroendocrinology* **20**, 26–34, <https://doi.org/10.1111/j.1365-2826.2008.01689.x> (2008).
36. Li, L. *et al.* Effect of oleoylethanolamide on diet-induced nonalcoholic fatty liver in rats. *J Pharmacol Sci* **127**, 244–250, <https://doi.org/10.1016/j.jphs.2014.12.001> (2015).
37. Ma, L., Guo, X. & Chen, W. Inhibitory effects of oleoylethanolamide (OEA) on H(2)O(2)-induced human umbilical vein endothelial cell (HUVEC) injury and apolipoprotein E knockout (ApoE^{-/-}) atherosclerotic mice. *Int J Clin Exp Pathol* **8**, 6301–6311 (2015).
38. Ma, Y. *et al.* Hyperlipidemia and atherosclerotic lesion development in Ldlr-deficient mice on a long-term high-fat diet. *PLoS One* **7**, e35835, <https://doi.org/10.1371/journal.pone.0035835> (2012).
39. Fan, A. *et al.* Atheroprotective effect of oleoylethanolamide (OEA) targeting oxidized LDL. *PLoS One* **9**, e85337, <https://doi.org/10.1371/journal.pone.0085337> (2014).
40. Jump, D. B., Depner, C. M., Tripathy, S. & Lytle, K. A. Impact of dietary fat on the development of non-alcoholic fatty liver disease in Ldlr^{-/-} mice. *Proc Nutr Soc* **75**, 1–9, <https://doi.org/10.1017/S002966511500244X> (2016).
41. Zhang, L. S. & Davies, S. S. Microbial metabolism of dietary components to bioactive metabolites: opportunities for new therapeutic interventions. *Genome Med* **8**, 46, <https://doi.org/10.1186/s13073-016-0296-x> (2016).
42. Bieghs, V. *et al.* LDL receptor knock-out mice are a physiological model particularly vulnerable to study the onset of inflammation in non-alcoholic fatty liver disease. *PLoS One* **7**, e30668, <https://doi.org/10.1371/journal.pone.0030668> (2012).
43. Kong, B., Luyendyk, J. P., Tawfik, O. & Guo, G. L. Farnesoid X receptor deficiency induces nonalcoholic steatohepatitis in low-density lipoprotein receptor-knockout mice fed a high-fat diet. *J Pharmacol Exp Ther* **328**, 116–122, <https://doi.org/10.1124/jpet.108.144600> (2009).
44. Ishibashi, S., Goldstein, J. L., Brown, M. S., Herz, J. & Burns, D. K. Massive xanthomatosis and atherosclerosis in cholesterol-fed low density lipoprotein receptor-negative mice. *J Clin Invest* **93**, 1885–1893, <https://doi.org/10.1172/JCI117179> (1994).
45. Tangirala, R. K., Rubin, E. M. & Palinski, W. Quantitation of atherosclerosis in murine models: correlation between lesions in the aortic origin and in the entire aorta, and differences in the extent of lesions between sexes in LDL receptor-deficient and apolipoprotein E-deficient mice. *J Lipid Res* **36**, 2320–2328 (1995).
46. Yu, E., Choe, G., Gong, G. & Lee, I. Expression of alpha-smooth muscle actin in liver diseases. *J Korean Med Sci* **8**, 367–373, <https://doi.org/10.3346/jkms.1993.8.5.367> (1993).
47. Nouchi, T., Tanaka, Y., Tsukada, T., Sato, C. & Marumo, F. Appearance of alpha-smooth-muscle-actin-positive cells in hepatic fibrosis. *Liver* **11**, 100–105 (1991).
48. Nie, Q. H. *et al.* Correlation between TIMP-1 expression and liver fibrosis in two rat liver fibrosis models. *World J Gastroenterol* **12**, 3044–3049 (2006).
49. Huang, Z. *et al.* Activation of peroxisome proliferator-activated receptor- α in mice induces expression of the hepatic low-density lipoprotein receptor. *British Journal of Pharmacology* **155**, 596–605, <https://doi.org/10.1038/bjp.2008.331> (2008).
50. Ngai, Y. F. *et al.* Ldlr^{-/-} mice display decreased susceptibility to Western-type diet-induced obesity due to increased thermogenesis. *Endocrinology* **151**, 5226–5236, <https://doi.org/10.1210/en.2010-0496> (2010).
51. Pepino, M. Y., Kuda, O., Samovski, D. & Abumrad, N. A. Structure-function of CD36 and importance of fatty acid signal transduction in fat metabolism. *Annu Rev Nutr* **34**, 281–303, <https://doi.org/10.1146/annurev-nutr-071812-161220> (2014).
52. Wilson, C. G. *et al.* Hepatocyte-Specific Disruption of CD36 Attenuates Fatty Liver and Improves Insulin Sensitivity in HFD-Fed Mice. *Endocrinology* **157**, 570–585, <https://doi.org/10.1210/en.2015-1866> (2016).
53. Pardina, E. *et al.* Hepatic CD36 downregulation parallels steatosis improvement in morbidly obese undergoing bariatric surgery. *International journal of obesity*, <https://doi.org/10.1038/ijo.2017.115> (2017).
54. Abu-Elheiga, L. *et al.* The subcellular localization of acetyl-CoA carboxylase 2. *Proc Natl Acad Sci USA* **97**, 1444–1449 (2000).
55. Harada, N. *et al.* Hepatic de novo lipogenesis is present in liver-specific ACC1-deficient mice. *Mol Cell Biol* **27**, 1881–1888, <https://doi.org/10.1128/MCB.01122-06> (2007).
56. Mao, J. *et al.* Liver-specific deletion of acetyl-CoA carboxylase 1 reduces hepatic triglyceride accumulation without affecting glucose homeostasis. *Proc Natl Acad Sci USA* **103**, 8552–8557, <https://doi.org/10.1073/pnas.0603115103> (2006).
57. Kim, C. W. *et al.* Acetyl CoA Carboxylase Inhibition Reduces Hepatic Steatosis but Elevates Plasma Triglycerides in Mice and Humans: A Bedside to Bench Investigation. *Cell Metab* **26**, 576, <https://doi.org/10.1016/j.cmet.2017.08.011> (2017).
58. Fan, C. Y. *et al.* Hepatocellular and hepatic peroxisomal alterations in mice with a disrupted peroxisomal fatty acyl-coenzyme A oxidase gene. *J Biol Chem* **271**, 24698–24710 (1996).
59. Fan, C. Y. *et al.* Steatohepatitis, spontaneous peroxisome proliferation and liver tumors in mice lacking peroxisomal fatty acyl-CoA oxidase. Implications for peroxisome proliferator-activated receptor alpha natural ligand metabolism. *J Biol Chem* **273**, 15639–15645 (1998).
60. Kohjima, M. *et al.* Re-evaluation of fatty acid metabolism-related gene expression in nonalcoholic fatty liver disease. *Int J Mol Med* **20**, 351–358 (2007).
61. Esposito, G. *et al.* Palmitoylethanolamide improves colon inflammation through an enteric glia/toll like receptor 4-dependent PPAR-alpha activation. *Gut* **63**, 1300–1312, <https://doi.org/10.1136/gutjnl-2013-305005> (2014).
62. Virmani, R., Burke, A. P., Kolodgie, F. D. & Farb, A. Vulnerable plaque: the pathology of unstable coronary lesions. *J Interv Cardiol* **15**, 439–446 (2002).
63. Moore, K. J. & Tabas, I. Macrophages in the pathogenesis of atherosclerosis. *Cell* **145**, 341–355, <https://doi.org/10.1016/j.cell.2011.04.005> (2011).
64. Haubenwallner, S. *et al.* Hypolipidemic activity of select fibrates correlates to changes in hepatic apolipoprotein C-III expression: a potential physiologic basis for their mode of action. *Journal of Lipid Research* **36**, 2541–2551 (1995).
65. Tavori, H. *et al.* Macrophage apoAI protects against dyslipidemia-induced dermatitis and atherosclerosis without affecting HDL. *Journal of Lipid Research* **56**, 635–643, <https://doi.org/10.1194/jlr.M056408> (2015).
66. Iacono, A., Raso, G. M., Canani, R. B., Calignano, A. & Meli, R. Probiotics as an emerging therapeutic strategy to treat NAFLD: focus on molecular and biochemical mechanisms. *J Nutr Biochem* **22**, 699–711, <https://doi.org/10.1016/j.jnutbio.2010.10.002> (2011).
67. Mimeo, M., Citorik, R. J. & Lu, T. K. Microbiome therapeutics - Advances and challenges. *Adv Drug Deliv Rev* **105**, 44–54, <https://doi.org/10.1016/j.addr.2016.04.032> (2016).

68. Faure, L. *et al.* Discovery and characterization of an Arabidopsis thaliana N-acylphosphatidylethanolamine synthase. *J Biol Chem* **284**, 18734–18741, <https://doi.org/10.1074/jbc.M109.005744> (2009).
69. Paigen, B., Morrow, A., Brandon, C., Mitchell, D. & Holmes, P. Variation in susceptibility to atherosclerosis among inbred strains of mice. *Atherosclerosis* **57**, 65–73 (1985).
70. Linton, M. F., Atkinson, J. B. & Fazio, S. Prevention of atherosclerosis in apolipoprotein E-deficient mice by bone marrow transplantation. *Science* **267**, 1034–1037 (1995).

Acknowledgements

We acknowledge Ling Ding and Youmin Zhang for technical assistance with animal euthanasia, cryo-sectioning, and aorta preparation, Dr. Arion Kennedy and C. Robb Flynn for helpful intellectual discussion in the pathogenesis of non-alcoholic fatty liver disease, the Vanderbilt MMPC for hepatic TG measurements, Vanderbilt Translational Pathology Shared Resource for liver histology staining and immunohistochemistry, and the Vanderbilt Digital Histology Shared Resource core for whole slide imaging and quantification of F4/80 immunostaining of liver sections. This work was supported by National Institutes of Health grant AT07830 (SSD), U24 DK059637 (MMPC), 2P30 CA068485-14 (VTPSR) and HL116263 (MFL).

Author Contributions

L.S.M., Z.C., P.G.Y., A.H.H., M.F.L., S.S.D. assisted in study concept and design of the studies. L.S.Z. collected and interpreted experimental data. L.S.M. assisted in tissue preparation, performed aortic, hepatic, and biochemical analyses, interpreted data, and prepared figures. N.S.D. performed mass spectrometric analyses on tissue NAPes. K.L.B. performed hepatic tissue staining and analyses. L.S.M. and S.D.D. drafted and revised the manuscript. P.G.Y., A.H.H., M.F.L. and S.S.D. assisted in analysis and interpretation of data, and provided critical reviews of the manuscript. M.F.L. and S.S.D. obtained project funding, provided technical and material support, supervised all aspects of the study, design, and execution. All authors reviewed the results and approved the final version of the manuscript.

Additional Information

Supplementary information accompanies this paper at <https://doi.org/10.1038/s41598-018-37373-1>.

Competing Interests: S.S.D. and Z.C. have a patent pending for the use of engineered bacteria expressing NAPE or NAE for treating obesity. S.S.D. receives funding from National Institutes of Health for studies using engineered bacteria.

Publisher's note: Springer Nature remains neutral with regard to jurisdictional claims in published maps and institutional affiliations.



Open Access This article is licensed under a Creative Commons Attribution 4.0 International License, which permits use, sharing, adaptation, distribution and reproduction in any medium or format, as long as you give appropriate credit to the original author(s) and the source, provide a link to the Creative Commons license, and indicate if changes were made. The images or other third party material in this article are included in the article's Creative Commons license, unless indicated otherwise in a credit line to the material. If material is not included in the article's Creative Commons license and your intended use is not permitted by statutory regulation or exceeds the permitted use, you will need to obtain permission directly from the copyright holder. To view a copy of this license, visit <http://creativecommons.org/licenses/by/4.0/>.

© The Author(s) 2019